CLNS 07/1989
CLEO 07-01

Measurement of the Decay Constant $f_{D_s^+}$ using $D_s^+ \to \ell^+\nu$

M. Artuso,[1] S. Blusk,[1] J. Butt,[1] S. Khalil,[1] J. Li,[1] N. Menaa,[1] R. Mountain,[1] S. Nisar,[1] K. Randrianarivony,[1] R. Sia,[1] T. Skwarnicki,[1] S. Stone,[1] J. C. Wang,[1] G. Bonvicini,[2] D. Cinabro,[2] M. Dubrovin,[2] A. Lincoln,[2] D. M. Asner,[3] K. W. Edwards,[3] P. Naik,[3] R. A. Briere,[4] T. Ferguson,[4] G. Tatishvili,[4] H. Vogel,[4] M. E. Watkins,[4] J. L. Rosner,[5] N. E. Adam,[6] J. P. Alexander,[6] D. G. Cassel,[6] J. E. Duboscq,[6] R. Ehrlich,[6] L. Fields,[6] L. Gibbons,[6] R. Gray,[6] S. W. Gray,[6] D. L. Hartill,[6] B. K. Heltsley,[6] D. Hertz,[6] C. D. Jones,[6] J. Kandaswamy,[6] D. L. Kreinick,[6] V. E. Kuznetsov,[6] H. Mahlke-Krüger,[6] D. Mohapatra,[6] P. U. E. Onyisi,[6] J. R. Patterson,[6] D. Peterson,[6] J. Pivarski,[6] D. Riley,[6] A. Ryd,[6] A. J. Sadoff,[6] H. Schwarthoff,[6] X. Shi,[6] S. Stroiney,[6] W. M. Sun,[6] T. Wilksen,[6] S. B. Athar,[7] R. Patel,[7] J. Yelton,[7] P. Rubin,[8] C. Cawlfield,[9] B. I. Eisenstein,[9] I. Karliner,[9] D. Kim,[9] N. Lowrey,[9] M. Selen,[9] E. J. White,[9] J. Wiss,[9] R. E. Mitchell,[10] M. R. Shepherd,[10] D. Besson,[11] T. K. Pedlar,[12] D. Cronin-Hennessy,[13] K. Y. Gao,[13] J. Hietala,[13] Y. Kubota,[13] T. Klein,[13] B. W. Lang,[13] R. Poling,[13] A. W. Scott,[13] A. Smith,[13] P. Zweber,[13] S. Dobbs,[14] Z. Metreveli,[14] K. K. Seth,[14] A. Tomaradze,[14] J. Ernst,[15] K. M. Ecklund,[16] H. Severini,[17] W. Love,[18] V. Savinov,[18] O. Aquines,[19] A. Lopez,[19] S. Mehrabyan,[19] H. Mendez,[19] J. Ramirez,[19] G. S. Huang,[20] D. H. Miller,[20] V. Pavlunin,[20] B. Sanghi,[20] I. P. J. Shipsey,[20] B. Xin,[20] G. S. Adams,[21] M. Anderson,[21] J. P. Cummings,[21] I. Danko,[21] D. Hu,[21] B. Moziak,[21] J. Napolitano,[21] Q. He,[22] J. Insler,[22] H. Muramatsu,[22] C. S. Park,[22] E. H. Thorndike,[22] and F. Yang[22]

(CLEO Collaboration)

[1] *Syracuse University, Syracuse, New York 13244*
[2] *Wayne State University, Detroit, Michigan 48202*
[3] *Carleton University, Ottawa, Ontario, Canada K1S 5B6*
[4] *Carnegie Mellon University, Pittsburgh, Pennsylvania 15213*
[5] *Enrico Fermi Institute, University of Chicago, Chicago, Illinois 60637*
[6] *Cornell University, Ithaca, New York 14853*
[7] *University of Florida, Gainesville, Florida 32611*
[8] *George Mason University, Fairfax, Virginia 22030*
[9] *University of Illinois, Urbana-Champaign, Illinois 61801*
[10] *Indiana University, Bloomington, Indiana 47405*
[11] *University of Kansas, Lawrence, Kansas 66045*
[12] *Luther College, Decorah, Iowa 52101*
[13] *University of Minnesota, Minneapolis, Minnesota 55455*
[14] *Northwestern University, Evanston, Illinois 60208*
[15] *State University of New York at Albany, Albany, New York 12222*
[16] *State University of New York at Buffalo, Buffalo, New York 14260*
[17] *University of Oklahoma, Norman, Oklahoma 73019*
[18] *University of Pittsburgh, Pittsburgh, Pennsylvania 15260*
[19] *University of Puerto Rico, Mayaguez, Puerto Rico 00681*
[20] *Purdue University, West Lafayette, Indiana 47907*
[21] *Rensselaer Polytechnic Institute, Troy, New York 12180*
[22] *University of Rochester, Rochester, New York 14627*

(Dated: August 17, 2007)

We measure the decay constant $f_{D_s^+}$ using the $D_s^+ \to \ell^+\nu$ channel, where the ℓ^+ designates either a μ^+ or a τ^+, when the $\tau^+ \to \pi^+\overline{\nu}$. Using both measurements we find $f_{D_s^+} = 274 \pm 13 \pm 7$ MeV. Combining with our previous determination of f_{D^+}, we compute the ratio $f_{D_s^+}/f_{D^+} = 1.23 \pm 0.11 \pm 0.04$. We compare with theoretical estimates.

PACS numbers: 13.20.Fc, 13.66.Bc

To extract precise information on the size of CKM matrix elements from B_d and B_s mixing measurements the ratio of "decay constants," that are related to the heavy and light quark wave-function overlap at zero separation, must be well known [1]. Recent measurement of B_s^0 mixing by CDF [2] has shown the urgent need for precise numbers. Decay constants have been calculated for both B and

D mesons using several methods, including lattice QCD [3]. Here we present the most precise measurement to date of $f_{D_s^+}$, and combined with our previous determination of f_{D^+} [4, 5], we find $f_{D_s^+}/f_{D^+}$.

In the Standard Model (SM) purely leptonic D_s decay proceeds via annihilation through a virtual W^+. The decay rate is given by [6]

$$\Gamma(D_s^+ \to \ell^+\nu) = \frac{G_F^2}{8\pi} f_{D_s^+}^2 m_\ell^2 M_{D_s^+} \left(1 - \frac{m_\ell^2}{M_{D_s^+}^2}\right)^2 |V_{cs}|^2 , \tag{1}$$

where $M_{D_s^+}$ is the D_s^+ mass, m_ℓ is the lepton mass, G_F is the Fermi constant, and $|V_{cs}|$ is a CKM matrix element with a value of 0.9738 [7].

In this Letter we report measurements of both $\mathcal{B}(D_s^+ \to \mu^+\nu)$ and $\mathcal{B}(D_s^+ \to \tau^+\nu)$, when $\tau^+ \to \pi^+\overline{\nu}$ ($D_s^+ \to \pi^+\overline{\nu}\nu$). More details are given in a companion paper [8]. The ratio $\Gamma(D_s^+ \to \tau^+\nu)/\Gamma(D_s^+ \to \mu^+\nu)$ predicted in the SM via Eq. 1 depends only on well-known masses, and equals 9.72; any deviation would be a manifestation of new physics as it would violate lepton universality [9]. New physics can also affect the expected widths; any undiscovered charged bosons would interfere with the SM W^+ [10].

The CLEO-c detector [11] is equipped to measure the momenta of charged particles, identify them using dE/dx and Cherenkov imaging (RICH) [12], detect photons and determine their directions and energies. We use 314 pb^{-1} of data produced in e^+e^- collisions using CESR near 4.170 GeV. Here the cross-section for our analyzed sample, $D_s^{*+}D_s^- + D_s^+D_s^{*-}$, is $\sim$1 nb. Other charm production totals $\sim$7 nb [13], and the underlying light-quark "continuum" is $\sim$12 nb. We fully reconstruct one D_s^- as a "tag," and examine the properties of the D_s^+. (Charge conjugate decays are used.) Track selection, particle identification, π^0, η, and K_S^0 criteria are the same as those described in Ref. [4], except that RICH identification now requires a minimum momentum of 700 MeV/c.

Tag modes are listed in Table I. For resonance decays we select intervals in invariant mass within $\pm$10 MeV of the known mass for $\eta' \to \pi^+\pi^-\eta$, $\pm$10 MeV for $\phi \to K^+K^-$, $\pm$100 MeV for $K^{*0} \to K^-\pi^+$, and $\pm$150 MeV for $\rho^- \to \pi^-\pi^0$. We require tags to have momentum consistent with coming from $D_sD_s^*$ production. The distribution for the $K^+K^-\pi^-$ mode (44% of all the tags) is shown in Fig. 1.

To select tags, we first fit the invariant mass distributions to the sum of two Gaussians centered at M_{D_s}. The r.m.s. resolution (σ) is defined as $\sigma \equiv f_1\sigma_1 + (1-f_1)\sigma_2$, where σ_1 and σ_2 are the individual widths and f_1 is the fractional area of the first Gaussian. We require the invariant masses to be within $\pm$ 2.5σ ($\pm 2\sigma$ for the $\eta\rho^-$ mode) of M_{D_s}. We have a total of 31302$\pm$472 tag candidates. Then we add a γ candidate that satisfies our shower shape requirement. Regardless of whether or not the γ forms a D_s^* with the tag, for real $D_s^*D_s$ events, the missing mass squared, MM^{*2}, recoiling against the γ and the D_s^- tag should peak at $M_{D_s^+}^2$. We calculate

$$\mathrm{MM}^{*2} = \left(E_{\rm CM} - E_{D_s} - E_\gamma\right)^2 - \left(\overrightarrow{p}_{\rm CM} - \overrightarrow{p}_{D_s} - \overrightarrow{p}_\gamma\right)^2,$$

where $E_{\rm CM}$ ($\overrightarrow{p}_{\rm CM}$) is the center-of-mass energy (momentum), E_{D_s} ($\overrightarrow{p}_{D_s}$) is the energy (momentum) of the fully reconstructed D_s^- tag, E_γ ($\overrightarrow{p}_\gamma$) is the en-

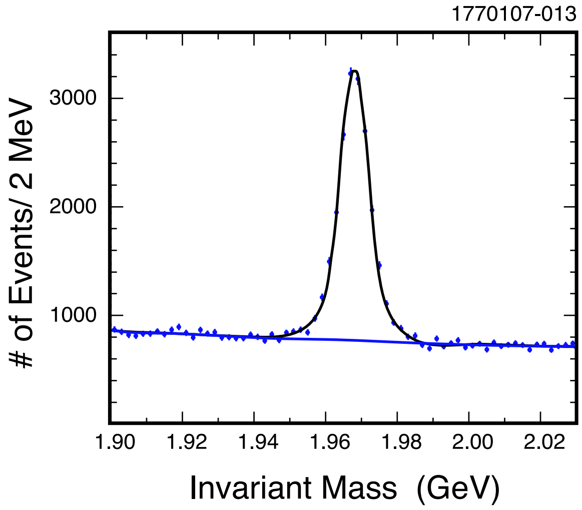

FIG. 1: Invariant mass of $K^+K^-\pi^-$ candidates after requiring the total energy to be consistent with the beam energy. The curve shows a fit to a two-Gaussian signal function plus a polynomial background.

TABLE I: Tagging modes and numbers of signal and background events, within cuts, from two-Gaussian fits to the invariant mass plots, and the number of γ tags in each mode, within $\pm 2.5\sigma$ from a fit to the signal Crystal Ball function (see text) and a 5th order Chebychev background polynomial and the associated background.

Mode	Invariant Mass		MM^{*2}	
	Signal	Bkgrnd	Signal	Bkgrnd
$K^+K^-\pi^-$	13871$\pm$262	10850	8053$\pm$ 211	13538
$K_S^0K^-$	3122$\pm$79	1609	1933$\pm$88	2224
$\eta\pi^-$	1609 $\pm$ 112	4666	1024$\pm$97	3967
$\eta'\pi^-$	1196$\pm$46	409	792$\pm$69	1052
$\phi\rho^-$	1678$\pm$74	1898	1050$\pm$113	3991
$\pi^+\pi^-\pi^-$	3654$\pm$199	25208	2300$\pm$187	15723
$K^{*-}K^{*0}$	2030$\pm$98	4878	1298$\pm$130	5672
$\eta\rho^-$	4142$\pm$281	20784	2195$\pm$225	17353
Sum	31302 $\pm$ 472	70302	18645$\pm$426	63520

ergy (momentum) of the additional γ. We use a kinematic fit that constrains the decay products of the D_s^- to M_{D_s} and conserves overall momentum and energy. All γ's in the event are used, except for those that are decay products of the D_s^- tag.

The MM^{*2} distribution from $K^+K^-\pi^-$ tags is shown in Fig. 2. We fit all the modes individually to determine the number of tag events. This procedure is enhanced by having information on the shape of the signal function. We use fully reconstructed $D_s^- D_s^{*+}$ events, and examine the signal shape when one D_s is ignored. The signal is fit to a Crystal Ball function [14], which determines σ and the shape of the tail. Though σ varies somewhat between modes, the tail parameters don't change, since they depend on beam radiation and γ energy resolution.

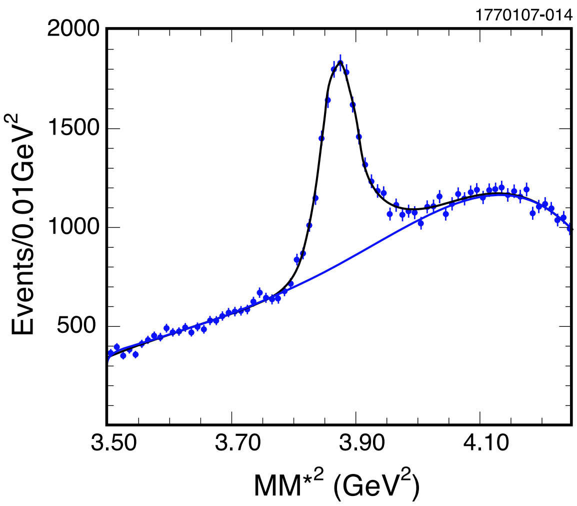

FIG. 2: The MM^{*2} distribution from events with a γ in addition to the $K^+K^-\pi^-$ tag. The curve is a fit to the Crystal Ball function and a 5th order Chebychev background function.

Fits of MM^{*2} in each mode when summed show 18645$\pm$426 events within a $\pm 2.5\sigma$ interval (see Table I). There is a small enhancement of (4.8 ± 1.0)% in our ability to find tags in $\mu^+\nu$ (or $\pi^+\overline{\nu}\nu$) events (tag bias) as compared with generic events. Additional systematic errors are evaluated by changing the fitting range, using 4th and 6th order Chebychev background polynomials, and allowing the parameters of the tail of the fitting function to float, leading to an overall systematic uncertainty of 5%.

Candidate $\mu^+\nu$ events are required to have only a single additional track oppositely charged to the tag with an angle $>35.9°$ with respect to the beam line. We also require that there not be any neutral energy cluster detected of more than 300 MeV, which is especially useful to reject $D_s^+ \to \pi^+\pi^0$ and $\eta\pi^+$ decays. Since here we are searching for events in which there is a single missing ν, the missing mass squared, MM^2, should peak at zero:

$$\begin{aligned} \text{MM}^2 = & \left(E_{\text{CM}} - E_{D_s} - E_\gamma - E_\mu\right)^2 \\ & - \left(\overrightarrow{p}_{\text{CM}} - \overrightarrow{p}_{D_s} - \overrightarrow{p}_\gamma - \overrightarrow{p}_\mu\right)^2 , \end{aligned} \quad (2)$$

where E_μ ($\overrightarrow{p}_\mu$) are the energy (momentum) of the candidate μ^+ track.

We also make use of a set of kinematical constraints and fit each event to two hypotheses: (1) the D_s^- tag is the daughter of a D_s^{*-} and (2) the D_s^{*+} decays into γD_s^+. The kinematical constraints, in the center-of-mass frame, are $\overrightarrow{p}_{D_s} + \overrightarrow{p}_{D_s^*} = 0$, $E_{\text{CM}} = E_{D_s} + E_{D_s^*}$, $E_{D_s^*} = E_{\text{CM}}/2 + \left(M_{D_s^*}^2 - M_{D_s}^2\right)/2E_{\text{CM}}$ or $E_{D_s} = E_{\text{CM}}/2 - \left(M_{D_s^*}^2 - M_{D_s}^2\right)/2E_{\text{CM}}$, $M_{D_s^*} - M_{D_s} = 143.6$ MeV. In addition, we constrain the invariant mass of the D_s^- tag to M_{D_s}. This gives a total of 7 constraints. The missing ν four-vector needs to be determined, so we are left with a three-constraint fit. We perform an iterative fit minimizing χ^2. To eliminate systematic uncertainties that depend on understanding the absolute scale of the errors, we do not make a χ^2 cut but simply choose the γ and the decay sequence in each event with the minimum χ^2.

We consider three separate cases: (i) the track deposits $<$ 300 MeV in the calorimeter, characteristic of a non-interacting pion or a μ^+; (ii) the track deposits $>$ 300 MeV in the calorimeter, characteristic of an interacting pion; or (iii) the track satisfies our electron selection criteria. The separation between muons and pions is not complete. Case (i) contains 99% of the muons but also 60% of the pions, while case (ii) includes 1% of the muons and 40% of the pions [5]. Case (iii) does not include any signal but is used for background estimation. For cases (i) and (ii) we insist that the track not be identified as an electron or a kaon. Electron candidates have a match between the momentum measured in the tracking system and the energy deposited in the CsI calorimeter, and dE/dx and RICH measurements consistent with this hypothesis.

For the $\mu^+\nu$ final state the MM^2 distribution is modeled as the sum of two Gaussians centered at zero. A Monte Carlo (MC) simulation of the MM^2 shows σ=0.025 GeV^2 after the fit. We check the resolution using the $D_s^+ \to \overline{K}^0 K^+$ mode. We search for events with at least one additional track identified as a kaon using the RICH detector, in addition to a D_s^- tag. The MM^2 resolution is 0.025 GeV^2 in agreement with the simulation.

In the $\pi^+\overline{\nu}\nu$ final state, the extra missing ν results in a smeared MM^2 distribution that is almost triangular in shape starting near -0.05 GeV^2, peaking near 0.10 GeV^2, and ending at 0.75 GeV^2.

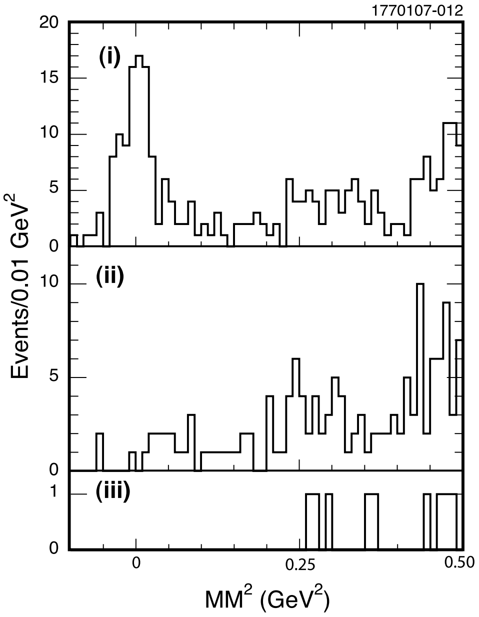

FIG. 3: The MM^2 distributions from data using D_s^- tags, and one additional opposite-sign charged track and no extra energetic showers, for cases (i), (ii), and (iii).

The MM^2 distributions from data are shown in Fig. 3. The overall signal region is -0.05 < MM^2 < 0.20 GeV^2. The upper limit is chosen to prevent background from $\eta\pi^+$ and $K^0\pi^+$ final states. The peak in Fig. 3(i) is due to $D_s^+ \to \mu^+\nu$. Below 0.20 GeV^2 in both (i) and (ii) we have $\pi^+\overline{\nu}\nu$ events. The specific signal regions are: for $\mu^+\nu$, $-0.05 <$ MM$^2 < 0.05$ GeV^2, corresponding to $\pm 2\sigma$; for $\pi^+\overline{\nu}\nu$, in case (i) $0.05 <$ MM$^2 < 0.20$ GeV^2 and in case (ii) $-0.05 <$ MM$^2 < 0.20$ GeV^2. In these regions we find 92, 31, and 25 events, respectively.

We consider backgrounds from two sources: one from real D_s^+ decays and the other from the background under the single-tag signal peaks. For the latter, we estimate the background from data using side-bands of the invariant mass, shown in Fig. 1. For case (i) we find 3.5 (properly normalized) background events in the $\mu^+\nu$ region and 2.5 backgrounds in the $\tau^+\nu$ region; for case (ii) we find 3 events. Our total background estimate summing over all of these cases is 9.0±2.3 events.

The background from real D_s^+ decays is evaluated by identifying specific sources. For $\mu^+\nu$ the only possible background is $D_s^+ \to \pi^+\pi^0$. Using a 195 pb^{-1} subsample of our data, we limit the branching fraction as $< 1.1 \times 10^{-3}$ at 90% C.L. [8]. This low rate coupled with the extra γ veto yields a negligible contribution. The real D_s^+ backgrounds for $\pi^+\overline{\nu}\nu$ are listed in Table II. Using the SM expected ratio of decay rates we calculate a contribution of 7.4 $\pi^+\overline{\nu}\nu$ events.

TABLE II: Event backgrounds in the $\pi^+\overline{\nu}\nu$ sample from real D_s^+ decays.

Source	$\mathcal{B}$(%)	case (i)	case (ii)	Sum
$D_s^+ \to X\mu^+\nu$	8.2	$0^{+1.8}_{-0}$	0	$0^{+1.8}_{-0}$
$D_s^+ \to \pi^+\pi^0\pi^0$	1.0	0.03±0.04	0.08±0.03	0.11±0.04
$D_s^+ \to \tau^+\nu$	6.4			
$\tau^+ \to \pi^+\pi^0\overline{\nu}$	1.5	0.55±0.22	0.64±0.24	1.20±0.33
$\tau^+ \to \mu^+\overline{\nu}\nu$	1.0	0.37±0.15	0	0.37±0.15
Sum		$1.0^{+1.8}_{-0}$	0.7±0.2	$1.7^{+1.8}_{-0.4}$

The event yield in the signal region, $N_{\rm det}$ (92), is related to the number of tags, $N_{\rm tag}$, the branching fractions, and the background $N_{\rm bkgrd}$ (3.5) as

$$\begin{aligned} N_{\rm det} - N_{\rm bkgrd} &= N_{\rm tag} \cdot \epsilon[\epsilon' \mathcal{B}(D_s^+ \to \mu^+\nu) \\ &\quad + \epsilon'' \mathcal{B}(D_s^+ \to \pi^+\overline{\nu}\nu)], \end{aligned} \tag{3}$$

where ϵ (80.1%) includes the efficiencies (77.8%) for reconstructing the single charged track including final state radiation, (98.3)% for not having another unmatched cluster in the event with energy greater than 300 MeV, and the correction for the tag bias (4.8%); ϵ' (91.4%) is the product of the 99.0% μ^+ calorimeter efficiency and the 92.3% acceptance of the MM^2 cut of $|$MM$^2| < 0.05$ GeV^2; ϵ'' (7.6%) is the fraction of $\pi^+\overline{\nu}\nu$ events contained in the $\mu^+\nu$ signal window (13.2%) times the 60% acceptance for a pion to deposit less than 300 MeV in the calorimeter. Using $\mathcal{B}(\tau^+ \to \pi^+\overline{\nu})$ of (10.90±0.07)% [7], the ratio of the $\pi^+\overline{\nu}\nu$ to $\mu^+\nu$ widths is 1.059; we find:

$$\mathcal{B}(D_s^+ \to \mu^+\nu) = (0.594 \pm 0.066 \pm 0.031)\%. \tag{4}$$

We can also sum the $\mu^+\nu$ and $\tau^+\nu$ contributions for $-0.05 <$ MM$^2 < 0.02$ GeV^2. Equation 3 still applies. The number of signal and background events changes to 148 and 10.7, respectively. ϵ' becomes 96.2%, and ϵ'' increases to 45.2%. The effective branching fraction, assuming lepton universality, is

$$\mathcal{B}^{\rm eff}(D_s^+ \to \mu^+\nu) = (0.638 \pm 0.059 \pm 0.033)\%. \tag{5}$$

The systematic errors on these branching fractions are dominated by the error on the number of tags (5%). Other errors include: (a) track finding (0.7%), determined from a detailed comparison of the simulation with double tag events where one track is ignored; (b) the error due to the requirement that the charged track deposit no more than 300 MeV in the calorimeter (1%), determined using two-body $D^0 \to K^-\pi^+$ decays [5]; (c) the γ veto efficiency (1%), determined by extrapolating measurements on fully reconstructed events. Systematic errors arising from the background estimates are negligible. The total systematic error for Eq. 4 is 5.2%, and is 5.1% for Eq. 5 as (b) doesn't apply here.

We also analyze the $\tau^+\nu$ final state independently. For case (i) we define the signal region to be the interval $0.05<\mathrm{MM}^2<0.20$ GeV^2, while for case (ii) $-0.05<\mathrm{MM}^2<0.20$ GeV^2. The upper limit on MM^2 is chosen to avoid background from the tail of the $K^0\pi^+$ peak. The fractions of the MM^2 range accepted are 32% and 45% for case (i) and (ii), respectively.

We find 31 [25] events in the signal region with a background of 3.5 [5.1] events for case (i) [(ii)]. The branching fraction, averaging the two cases is

$$\mathcal{B}(D_s^+ \to \tau^+\nu) = (8.0 \pm 1.3 \pm 0.4)\%, \qquad (6)$$

where the systematic error includes a contribution of 0.06% from the uncertainty on $\mathcal{B}(\tau^+ \to \pi^+\overline{\nu})$. We measure $13.4 \pm 2.6 \pm 0.2$ for the ratio of $\tau^+\nu$ to $\mu^+\nu$ rates using Eq. 4. Here the systematic error is dominated by the uncertainty on the minimum ionization cut. We also set an upper limit of $\mathcal{B}(D_s^+ \to e^+\nu) < 1.3 \times 10^{-4}$ at 90% C.L. Both of these results are consistent with SM predictions and lepton universality.

We perform an overall check of our procedures by measuring $\mathcal{B}(D_s^+ \to \overline{K}^0 K^+)$. We compute the MM^2 (Eq. 2) using events with an additional charged track identified as a kaon. These track candidates have momenta of approximately 1 GeV/c; here the RICH has a pion to kaon fake rate of 1.1% with a kaon detection efficiency of 88.5% [12]. For this study, we do not veto events with extra charged tracks, or γ's, because of the presence of the K^0. We determine $\mathcal{B}(D_s^+ \to \overline{K}^0 K^+) = (2.90 \pm 0.19 \pm 0.18)\%$. This method gives a result in good agreement with preliminary CLEO-c results using double tags of $(3.00 \pm 0.19 \pm 0.10)\%$ [15]; these results are not independent.

We also performed the entire analysis on a MC sample that is 4 times larger than the data sample. The input branching fraction is 0.5% for $\mu^+\nu$ and 6.57% for $\tau^+\nu$, while our analysis measured $(0.514\pm0.027)\%$ for the case (i) $\mu^+\nu$ signal and $(0.521\pm0.024)\%$ for $\mu^+\nu$ and $\tau^+\nu$ combined.

Using $\mathcal{B}(D_s^+ \to \mu^+\nu)$ from Eq. 5, and Eq. 1 with a D_s lifetime of $(500\pm7)\times10^{-15}$ s [7], we extract

$$f_{D_s^+} = 274 \pm 13 \pm 7 \text{ MeV}. \qquad (7)$$

We combine with our previous result $f_{D^+} = 222.6 \pm 16.7^{+2.8}_{-3.4}$ MeV [4], and find

$$f_{D_s^+}/f_{D^+} = 1.23 \pm 0.11 \pm 0.04. \qquad (8)$$

Lattice QCD predictions for $f_{D_s^+}$ and the ratio $f_{D_s^+}/f_{D^+}$ have been summarized by Onogi [16]. Our measurements are consistent with most calculations; examples are unquenched Lattice that predicts $249\pm 3\pm16$ MeV and $1.24\pm0.01\pm0.07$ for the ratio [17], while a recent quenched prediction gives $266\pm10\pm 18$ MeV and $1.13\pm0.03\pm0.05$ [18]. There is no evidence yet for any suppression in the ratio due to the presence of a virtual charged Higgs [10].

The CLEO-c determination of $f_{D_s^+}$ is the most accurate to date and consistent with other measurements [7, 8]. It also does not rely on the independent determination of any normalization mode (e.g. $\phi\pi^+$). (We note that a preliminary CLEO-c result using $D_s^+ \to \tau^+\nu$, $\tau^+ \to e^+\overline{\nu}\nu$ [19] is consistent with these results.)

We gratefully acknowledge the effort of the CESR staff in providing us with excellent luminosity and running conditions. This work was supported by the A.P. Sloan Foundation, the National Science Foundation, the U.S. Department of Energy, and the Natural Sciences and Engineering Research Council of Canada.

[1] G. Buchalla, A. J. Buras and M. E. Lautenbacher, Rev. Mod. Phys. **68**, 1125 (1996).
[2] A. Abulencia *et al.* (CDF), Phys. Rev. Lett. **97**, 242003 (2006). See also V. Abazov *et al.* (D0), Phys. Rev. Lett. **97**, 021802 (2006).
[3] C. Davies *et al.*, Phys. Rev. Lett. **92**, 022001 (2004).
[4] M. Artuso *et al.* (CLEO), Phys. Rev. Lett. **95**, 251801 (2005).
[5] G. Bonvicini *et al.* (CLEO) Phys. Rev. **D70**, 112004 (2004).
[6] D. Silverman and H. Yao, Phys. Rev. **D38**, 214 (1988).
[7] W.-M. Yao *et al.*, J. Phys. **G33**, 1 (2006).
[8] T. K. Pedlar *et al.* (CLEO), arXiv:0704.0437[hep-ex], submitted to Phys. Rev. **D**.
[9] J. Hewett, [hep-ph/9505246]; W.-S. Hou, Phys. Rev. **D48**, 2342 (1993).
[10] A. G. Akeroyd, Prog. Theor. Phys. **111**, 295 (2004).
[11] D. Peterson *et al.*, Nucl. Instrum. and Meth. **A478**, 142 (2002); Y. Kubota *et al.*, Nucl. Instrum. and Meth. **A320**, 66 (1992).
[12] M. Artuso *et al.*, Nucl. Instrum. Meth. **A554**, 147 (2005).
[13] R. Poling, [hep-ex/0606016].
[14] P. Rubin *et al.* (CLEO), Phys. Rev. **D73**, 112005 (2006).

[15] N. E. Adam *et al.* (CLEO), [hep-ex/0607079].
[16] T. Onogi [hep-lat/0610115].
[17] C. Aubin *et al.*, Phys. Rev. Lett. **95**, 122002 (2005).
[18] T. W. Chiu *et al.*, Phys. Lett. **B624**, 31 (2005).
[19] S. Stone [hep-ex/0610026].